

**NUMERICAL INVESTIGATION OF FLAT PLATE FIN HEAT SINK CONFIGURATIONS UNDER FORCED CONVECTION: A COMPARATIVE CFD STUDY**

Doaa Fadhil Kareem 1,
Hasan F Abd Ali 2,
Sajjad Ali3*

1Al -Mussaib Technical College,
Al -Furat Al -Awsat Technical University, Babylon 51006, Iraq
doaa.fadhil.tcm@atu.edu.iq

2Center for Research on Environment and Renewable Energy,
University of Kerbela, Iraq
hasan.flayyih@uokerbala.edu.iq

3Al -Mussaib Technical College,
Al -Furat Al -Awsat Technical University, Babylon 51006, Iraq
sajjad.habib.tcm@atu.edu.iq

Abstract

The effectiveness of air-cooled plate-fin heat sinks is limited by the gradual buildup of the thermal boundary layer on typical flat fin surfaces, and these heat sinks are increasingly used for effective thermal control of electronic systems. In the present study, the performance of a conventional flat plate fin heat sink with three geometric modifications is systematically investigated using the three-dimensional computational fluid dynamics. The modifications include a tapered fin with a draft angle of 5 degree, a notched fin with five alternating rectangular slots, and a perforated fin with twelve circular through-holes. The base plate dimensions, fin height and fin count are same for all the four configurations. The four configurations are simulated in ANSYS Fluent 2022 R1 with realizable k-epsilon turbulence model and conjugate heat transfer with uniform velocity of 3 m/s at inlet, inlet temperature of 300 K and base heat flux of 10000 W/m². The tapered fin yields the maximum heat transfer coefficient (169.38 W/m²K, +6.4% from the flat plate reference) and is the only Performance Evaluation Criterion over unity (PEC = 1.004) even with a 19% increase in pressure drop. The perforated and notched fins have the PECs of 0.983 and 0.962, respectively. This means that their hydraulic penalties are not completely compensated by the thermal benefits for the given geometric parameters. The temperature contour analysis shows that the notched fin has the highest peak temperature (81.1 °C) owing to the flow recirculation in the notch cavities and highly interrupted conduction channel. The results show that the tapered fin profile has the best overall thermo-hydraulic performance of all the configurations investigated and may give useful guidelines for the design of forced air-cooled electronic heat sinks.

Keywords: Plate-fin heat sink; Forced convection; CFD; Tapered fin; Perforated fin; Notched fin; Performance Evaluation Criterion.

Introduction

The miniaturization of electronic components along with the ever-expanding processing capability of chips has made the heat management a major engineering problem in the area of current electronic design [1]. The density of transistors is growing, and the operating clock frequencies are increasing. The amount of heat generated internally by mainstream semiconductor devices like processors and power amplifiers is increasing and traditional passive cooling methods are no longer able to handle this thermal load effectively [2]. Uncontrolled heat buildup in electronic systems degrades device performance, increases material fatigue, and is the major factor in premature system failure. Industry third-party estimates reveal that a high majority of component failures are caused by heat. Reliable heat dissipation is a fundamental design criterion, not a supplementary factor [3]. According to the thermal management heat dissipation requirements mentioned in the previous paragraph, many high-end cooling technologies have been developed so far, such as sophisticated liquid cooling loops, thermoelectric coolers, phase-change systems and jet impingement setups. However, extended surface air-cooling heat sinks still dominate the market because of simple form, good mechanical dependability, cheap cost, and simplicity of integration. The main advantage of the widespread use of the immobile fluid interface system discussed in this study is that it removes three dangers associated with conventional liquid systems, namely, leakage, corrosion and pump failure [4].

This paper first explains the basic working principle of heat sinks: heat sinks minimize the thermal resistance between the heat source and the surrounding environment by increasing the effective contact surface area with the cooling fluid. Fans or blowers are used to cause air to flow through the fin array under forced convection working conditions. The fins transmit heat from the heating substrate to the flowing air stream via a combination of heat conduction and convection. The structure of the fin is the main influencing factor. This is because it impacts both the accessible heat exchange area and the fluid dynamic conditions of the fin channels [5]. Traditional flat plate fins are easy to manufacture and widely used, but there are inherent limitations of the thermal performance. As the air flows over the surface of the fin, the thermal boundary layer becomes thicker in the flow direction, which results in a continuous decrease of the convective heat transfer coefficient and a non-uniform temperature distribution. Moreover, the total thermal efficiency of a fin decreases significantly with the increase of the fin length [6]. The flat plate fins cannot attain the inherent theoretical heat dissipation potential. The theoretical top limit of the heat dissipation of the material of flat plate fins is somewhat different from the actual heat dissipation in engineering practice.

The bottleneck of heat transfer efficiency in the present industrial heat dissipation systems has promoted a wave of study in the area of fin geometry modification. The existing research has developed along three key optimization routes, which describe the three mainstream modification procedures that have received the most attention from scholars. Conical fins are one of these solutions that may improve heat transfer performance by controlling flow field distribution. The current research context collation has created the basic framework for the future scheme design [7]. Notched or slotted fins provide periodic discontinuities which cause the thermal boundary layer to regenerate again and again. This leads to retain a high local heat transfer coefficient all along the height of the fin, with a little increase of the flow resistance [8]. Perforated fins may lead to the formation of secondary flows, vortex shedding and local flow acceleration in the neighborhood of each hole, hence improving heat transmission and mixing without any extra energy expenditure [9]. The physical processes of all sorts of thermal enhancement

retrofits are individual, and the evaluation under the uniform circumstances is necessary to support the reasonable selection of engineering design plans.

In the last decade, there has been substantial study on the thermohydraulic performance of plate-fin radiators among the academic community. These studies mainly concentrate on the effect of geometric parameters and surface changes on the heat transfer and flow characteristics, and the sub-classification of geometric parameters will be discussed in the coming sections. Adhikari et al. [10] performed three-dimensional CFD simulations based on ANSYS Fluent. They revealed that fin height, thickness and spacing have non-trivial joint effects on Nusselt number and pressure drop, and identical fin surface area is not a guarantee of similar thermal performance. Ashour et al. [11] used the combination of numerical simulations and experimental analysis. Their study on air-cooled thermoelectric systems indicated that fin amount and height had a substantial influence on thermal resistance and hydraulic loss of the system. Increasing heat transfer area and increasing flow channel obstruction might result in an ideal setup. Thus, the geometric optimization of plate-fin heat sinks is not a single parameter consideration, but should include the linked nature of thermal response and hydrodynamic response.

Based on this study basis indicated above, a new research strand of surface modification on plate-fin heat sinks has been developed in recent years in this sector, and the main objective is to break thermal boundary layers and enhance local convection. Two relevant, complimentary research have been published one after another. Shaeri et al., [6] carried out a conjugate heat transfer analysis of modified plate-fin heat sinks with perforations and slots and found that the heat transfer coefficient for both configurations was greater than the conventional plain fins while inducing a lower pressure drop than the reference solid fins. The reason for this performance gain is less flow restriction due to eliminated material. This unexpected finding suggests that updated setups should be assessed by utilizing full thermal-hydraulic measures rather than thermal performance just. In a work supplementary to this, Ghandouri et al., [5] improved the perforation design of rectangular plate-fin heat sinks for both natural and forced convection. The research compares the performance of circular, square and triangular perforations with equal projected area. It has been observed that square perforations improve the heat transfer coefficient up to 44% as compared to unperforated fins under forced convection. The study revealed that the ideal perforation shape relies on the dominant operating flow circumstances, which suggests that operating conditions must be properly described when a perforation design is selected.

In the examination of fin profile alterations a different but equally beneficial way has been undertaken. Li et al., [12] developed the ribbed flat-plate wing structure based on the shape of placoid scales. Verification by numerical simulation and optimization shows that these ribs can trigger reattachment of separated boundary layers, and improve convective performance in the low-Reynolds-number range. The net benefit of these ribs exceeds their associated hydraulic cost over a broad range of operating conditions. Arjunan and Kumaresan [7] performed an experimental investigation on fin heat exchange, especially on converging fins, to validate the real thermal performance of this fin type. It is rather obvious from the present research that spanwise geometric modification of fins may be an efficient means to increase overall heat transfer performance of fins.

In recent years, many studies have carried out combined optimization explorations targeting the aforementioned heat dissipation principles. Maji et al., [13]. used a three-dimensional CFD approach coupled with particle swarm optimization and the teaching-learning-based optimization algorithm to study heat sinks with conical perforated pin fins. They found that fins with inward-converging

perforations delivered a maximum performance improvement of 6.1% compared to equivalent non-conical heat sinks of the same type, and the internal taper of perforations is the core controlling factor for local flow field distribution. Zohora et al. [14] conducted a numerical study using the realizable k-epsilon turbulence model to investigate an innovative perforated pin fin design. They noted that the impact of perforation configuration and arrangement on thermal performance is far greater than that of perforation size itself, and the Nusselt number improvement brought by staggered arrangements always outperforms that of in-line layouts, Muneeshwaran et al. [15] organizes and summarizes various topological configurations of microchannel heat sinks, and proposes that a full-domain conical fin arrangement can achieve optimal temperature uniformity. The advantages of this arrangement stem from a larger heat dissipation area and stronger local fluid mixing; their conclusion is applicable across scales. While a large body of related work has been accumulated in the field of flat plate fin improvement strategies, none of the current studies have systematically compared the three mainstream modification schemes—tapering, grooving, and perforating—under a unified framework that shares the same baseline geometry, boundary conditions, and performance evaluation system. Furthermore, existing research has clear deficiencies: studies only investigate a single type of modification, adopt inconsistent conditions, and fail to assess hydraulic losses concurrently. The study by Pires-Fonseca and Carrasco-Altemani [16] research on flat plate fin and strip fin heat sinks noted that the field of thermal management lacks comparative analyses of multiple geometric configurations conducted under unified, controlled-variable conditions. This shortcoming makes it impossible to screen out the optimal scheme for improving thermo-hydraulic equilibrium.

In this work, three-dimensional CFD numerical simulations of flat fin heat sinks are carried out for thermal management of air-cooled electronic devices under forced convection circumstances. The traditional flat fins are used as the baseline group, and three modified fin designs are constructed in tandem as the experimental groups. All heat sinks have common fundamental specifications, including base plate size of 100×100 mm, fin height of 40 mm and 7 fins per heat sink. All boundary conditions are same for all situations. The three experimental groups are as follows: (1) tapered fins with a draft angle of 5° (root thickness 6 mm, tip thickness 2 mm); (2) slotted fins with 5 sets of staggered rectangular slots (slot width 8 mm, slot depth 8 mm); (3) perforated fins with 12 evenly distributed circular holes (hole diameter 6 mm, 4 columns and 3 rows). In this work, the simulation tool of ANSYS Fluent is used to explore the effects of working parameters, i.e. intake air velocity of 2 m/s, inlet temperature of 300 K, base plate heat flux of 20000 W/m², on the thermal performance of the heat sink using the realizable k-epsilon turbulence model with improved wall treatment. Core indications such as outlet temperature, average convective heat transfer coefficient, Nusselt number and pressure drop across the fin array are retrieved post simulations. The same performance assessment criteria balancing the thermal gain with the hydraulic cost is used to choose the ideal configuration.

2. NUMERICAL ANALYSIS

2.1 Geometry Design and CAD Modelling

This study conducted pre-modeling for thermal simulation targeting four types of flat fin heat sinks. All four adopt the same basic structure of an aluminum substrate paired with 7 fins. The flow field domain is set as a closed rectangular domain measuring 125mm wide \times 80mm high \times 1100mm long. The fin array is arranged at the center of the domain, with 500mm of flow channel length reserved for both the

upstream and downstream sections. All basic geometric parameters are uniformly fixed, with only fin surface modification retained as the sole variable. The visualization diagrams of the four configurations correspond to Figure 1, and their parameter table corresponds to Table 1.

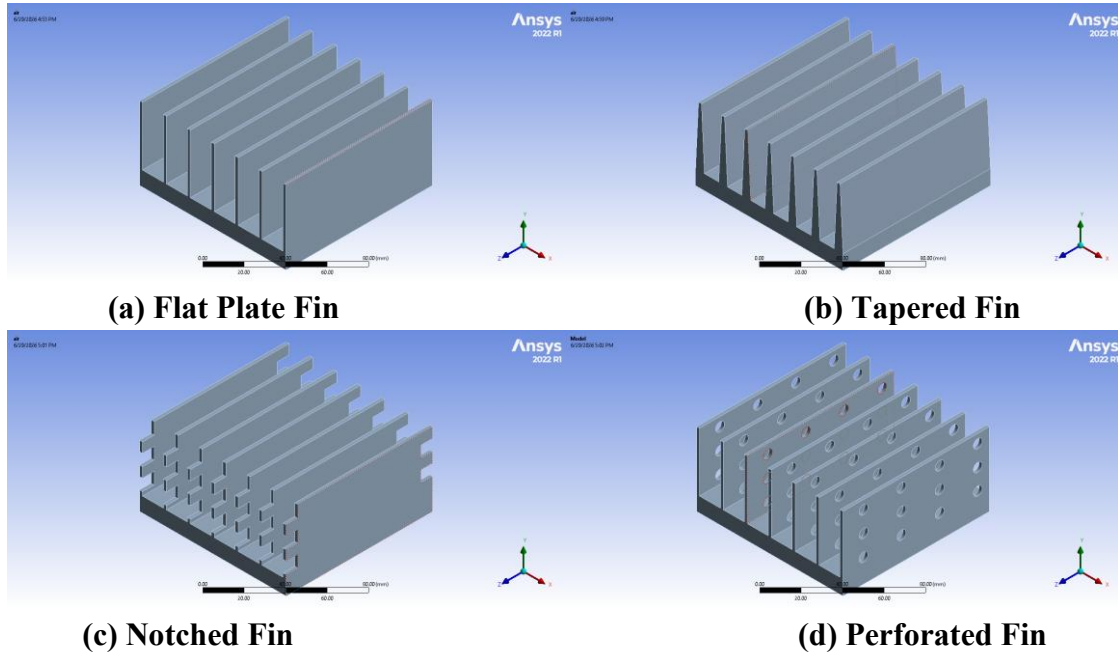


Figure 1. CAD models of the four fin configurations: (a) flat plate, (b) tapered, (c) notched, (d) perforated.

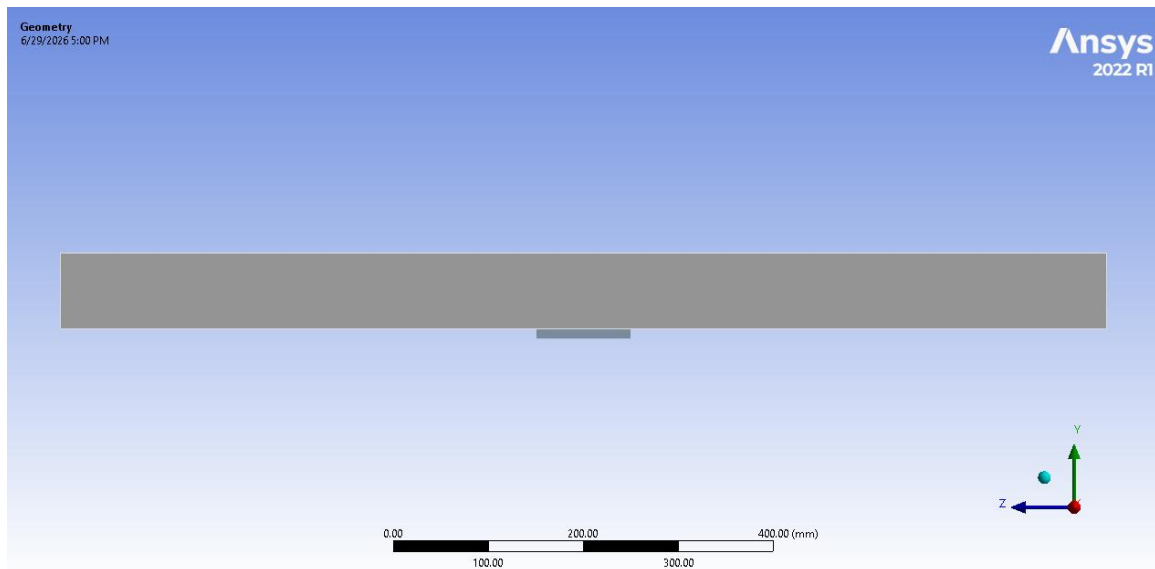


Figure 2. Fluid domain with the fin array centred at $Z = 500$ mm within the 1,100 mm channel.



Table 1. Geometric parameters of all fin configurations.

Parameter	Flat Plate	Tapered	Notched	Perforated
Base plate (L×W×t, mm)	100×100×5	100×100×5	100×100×5	100×100×5
Fin height H (mm)	40	40	40	40
Fin length L (mm)	100	100	100	100
Tip thickness t_t (mm)	2	2	2	2
Base thickness t_b (mm)	2	6	2	2
Draft angle θ	—	5°	—	—
Notch size (mm)	—	—	8×8	—
No. of notches	—	—	5 (alternating)	—
Hole diameter D (mm)	—	—	—	6
No. of holes	—	—	—	12 (4×3)
No. of fins	7	7	7	7
Fin pitch (mm)	16.3	16.3	16.3	16.3
Inter-fin gap (mm)	14.3	10.3	14.3	14.3

2.2 Mesh Generation

ANSYS Meshing 2022 R1 is used to generate the computational grids for numerical simulation. The solid fin domain adopts structured hexahedral grids to minimize numerical diffusion, while the fluid domain uses unstructured tetrahedral grids. An inflation layer is set at the solid-liquid interface, with a first layer height of 0.1 mm, a growth rate of 1.2, and a maximum of 8 layers. The grid size on all fin surfaces is set to 1 mm. For the reference flat plate, the number of grid elements, faces, and nodes are 1478957, 3096366, and 276375 respectively. A detailed schematic of the grid is shown in Figure 3.

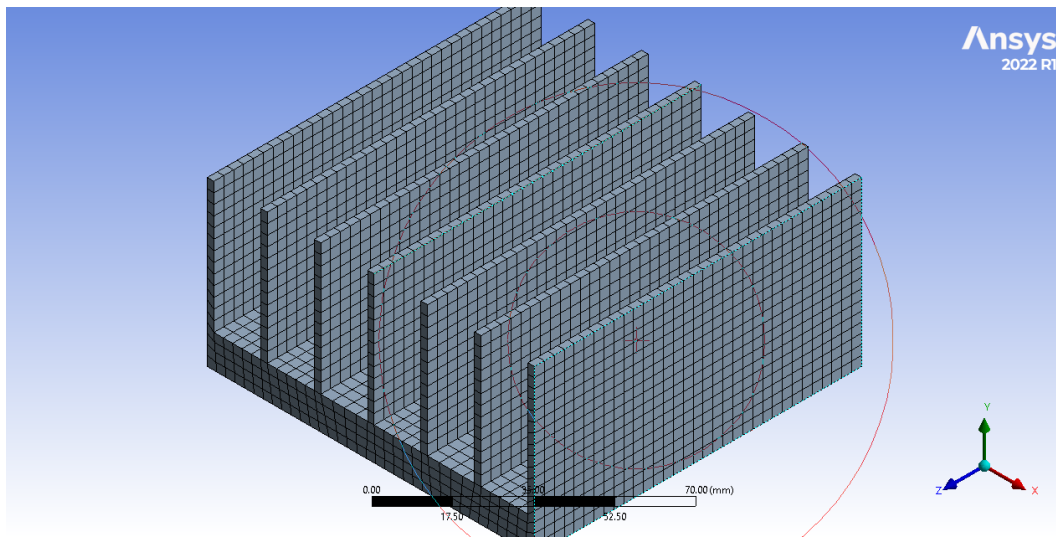


Figure 3. Computational mesh showing hexahedral elements on the solid fin domain and inflation layers at the solid–fluid interface.

2.3 Boundary Conditions

This study established unified boundary conditions for all four groups of conjugate flow-heat transfer numerical simulations, with all parameters documented in Table 2 and Table 4. A velocity inlet boundary

was assigned to the channel inlet, with a flow velocity of 3 m/s, temperature of 300 K, turbulence intensity of 5%, and viscosity ratio of 10. The channel outlet was set to a zero-gauge pressure. A heat flux of 10000 W/m² was applied to the lower surface of the substrate. The fin-fluid interface adapted for conjugate heat transfer was configured as a coupled thermal wall, and all remaining walls were set as adiabatic no-slip walls.

Table 2. Applied boundary conditions.

Boundary	Type	Condition	Value
Inlet	Velocity Inlet	Velocity / Temperature	3 m/s / 300 K
Inlet	Turbulence	Intensity / Viscosity ratio	5% / 10
Outlet	Pressure Outlet	Gauge pressure	0 Pa
Base plate (heater)	Wall — Heat Flux	Heat flux	10,000 W/m ²
Fin surfaces	Wall — Coupled	Conjugate heat transfer	Enabled
Channel walls	Wall — Adiabatic	Heat flux	0 W/m ²

Table 3. Thermophysical properties of air and aluminium.

Property	Symbol	Air	Aluminium
Density	ρ (kg/m ³)	1.225	2,719
Specific heat	C_p (J/kg·K)	1,006.43	871
Thermal conductivity	k (W/m·K)	0.0242	202.4
Dynamic viscosity	μ (kg/m·s)	1.789×10^{-5}	—

2.4 CFD Simulation Methodology

The numerical simulations conducted in this study used ANSYS Fluent 2022 R1, a three-dimensional steady-state pressure-based solver, paired with the realizable k- ϵ turbulence model equipped with enhanced wall treatment. The hydraulic diameter of the inter-fin channel is defined as:

$$D_h = \frac{2sH}{s+H} \quad (1)$$

where s is the inter-fin gap and H is the fin height, giving $D_h = 21.1$ mm. The channel Reynolds number $Re = \rho V D_h / \mu \approx 2,880$ at $V = 2$ m/s, confirming turbulent flow. The governing equations are:

Continuity equation[17] :

$$\frac{\partial u_i}{\partial x_i} = 0 \quad (2)$$

Reynolds-averaged Navier–Stokes (RANS) momentum equation[17]:

$$\rho u_j \frac{\partial u_i}{\partial x_j} = -\frac{\partial P}{\partial x_i} + \frac{\partial}{\partial x_j} \left[\mu \frac{\partial u_i}{\partial x_j} - \rho u'_i u'_j \right] \quad (3)$$

Energy equation for the fluid domain[18]:

$$\rho u_j \frac{\partial T}{\partial x_j} = \frac{\partial}{\partial x_j} \left[\left(\frac{\lambda}{C_p} + \frac{\mu_t}{Pr_t} \right) \frac{\partial T}{\partial x_j} \right] \quad (4)$$

Energy equation for the solid aluminium domain (conjugate heat transfer) [18]:

$$\frac{\partial}{\partial x_i} \left[k_s \frac{\partial T}{\partial x_i} \right] = 0 \quad (5)$$

Realizable k- ϵ turbulence model transport equations [19]:

$$\frac{\partial}{\partial x_j} (\rho u_j k) = \frac{\partial}{\partial x_j} \left[\left(\mu + \frac{\mu_t}{\sigma_k} \right) \frac{\partial k}{\partial x_j} \right] + G_k - \rho \epsilon \quad (6)$$



$$\frac{\partial}{\partial x_j} (\rho u_j \varepsilon) = \frac{\partial}{\partial x_j} \left[\left(\mu + \frac{\mu_t}{\sigma_\varepsilon} \right) \frac{\partial \varepsilon}{\partial x_j} \right] + C_1 S \varepsilon - C_2 \frac{\rho \varepsilon^2}{k + \sqrt{v \varepsilon}} \quad (7)$$

where G_k is the turbulence production term and model constants are $C_1 \varepsilon = 1.44$, $C_2 = 1.9$, $\sigma_k = 1.0$, $\sigma_\varepsilon = 1.2$ [19].

The SIMPLE algorithm was used with second-order upwind discretization. Convergence criteria: 10^{-4} for continuity, velocity, and turbulence; 10^{-7} for energy.

3. RESULTS AND DISCUSSION

3.1 Temperature Distribution

Figure 4 shows the temperature contour cloud plot of the heat conduction simulation result for four plate-fin designs. The thermal performance of all four kinds of fins is distinguishable, and they obey the same basic rule of heat conduction: The highest temperature of the flat fin is 74.4°C , with a smooth temperature gradient due to the undisturbed expansion of the boundary layer, while the maximum temperature of the conical fin is 78.2°C , with high temperatures localized near the fin root. [7], this feature is ascribed to the thick root cross-section that increases the local conduction flux and the converging channel that sustains the fin tip at a low temperature; the perforated fin has a maximum temperature of 78.7°C , with local cold spots formed at the perforations, which is mainly because of the eddy induced mixing. The lower solid cross-section results in increased temperatures in all other locations [8]. The notched fin has a maximum temperature of 81.1°C with poor thermal uniformity. This is due to backflow inside the notch cavity and interrupted heat conduction routes.

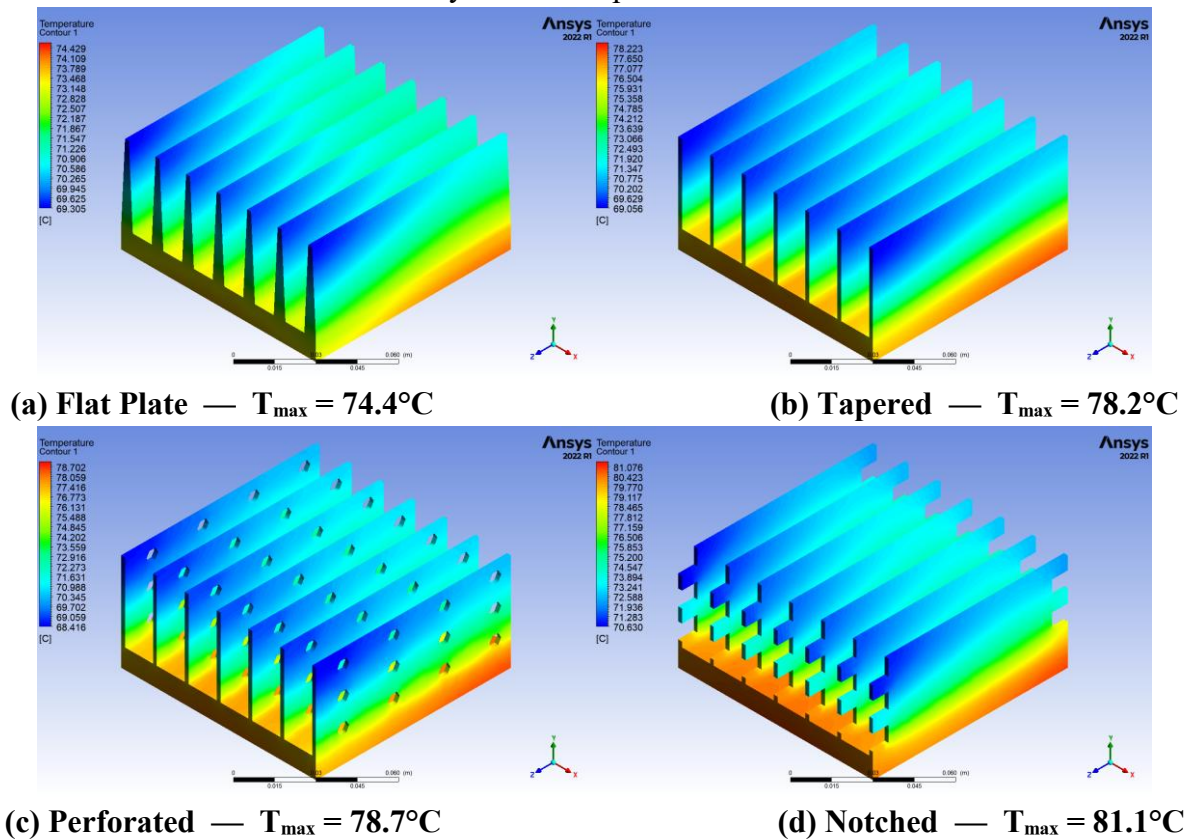


Figure 4. Temperature contour maps ($V = 2 \text{ m/s}$, $q'' = 20,000 \text{ W/m}^2$, $T_{\text{in}} = 300 \text{ K}$).

3.2 Quantitative Performance Comparison

The complete performance metrics are summarized in Table 4. Each metric is discussed individually below with its corresponding bar chart.

Table 4. Thermal-hydraulic performance of the four fin configurations.

Configuration	h ($W/m^2 \cdot K$)	Nu	ΔP (Pa)	PEC
Flat Plate (Ref.)	159.16	138.77	4.217	1.000
Tapered Fin	169.38	147.69	5.016	1.004
Perforated Fin	158.01	137.77	4.351	0.983
Notched Fin	152.17	132.68	4.135	0.962

3.2.1 Heat Transfer Coefficient

Figure 5 Taking the convection heat transfer coefficient of the baseline flat plate, which is $159.16 W/m^2 \cdot K$, as the reference, the coefficient h of the conical fin is measured at $169.38 W/m^2 \cdot K$, marking a 6.4% increase over the baseline. The mechanism through which its converging flow channel accelerates airflow is corroborated by Arjunan et al. [7]. The h values of the perforated fin and the slotted fin are $158.01 W/m^2 \cdot K$ and $152.17 W/m^2 \cdot K$ respectively. The slotted fin's h is 4.4% lower than the baseline, a result of weakened heat conduction outweighing the improvement in convection.

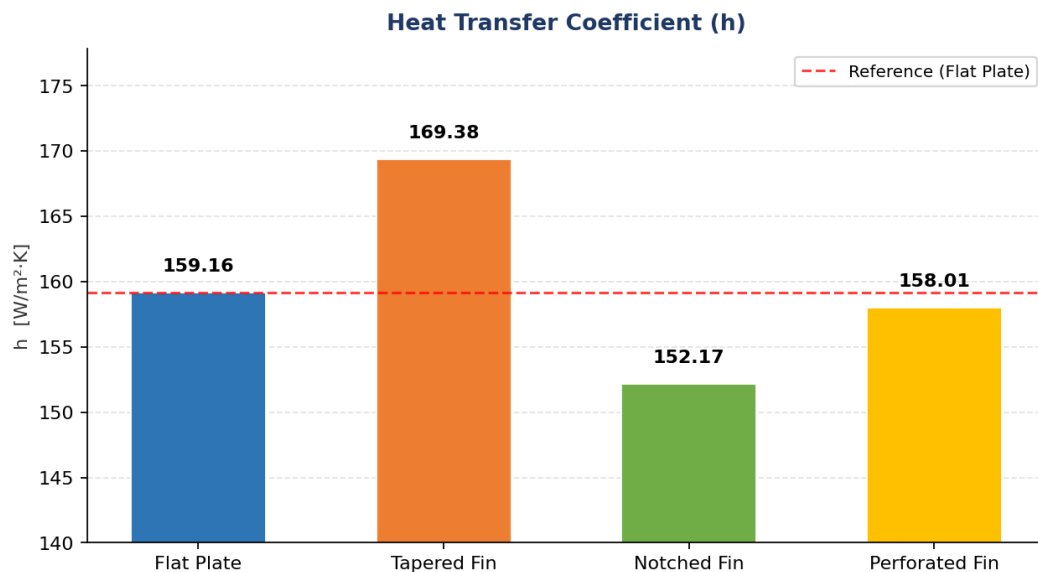


Figure 5. Average heat transfer coefficient h . Dashed line = flat plate reference.

3.2.2 Nusselt Number

the variation in Nusselt numbers of the three types of fins analyzed (Figure 6) aligns with the theoretical expectations of Equation (9). The measured Nu (Nusselt number) of the conical fin is 147.69, which is 6.4% higher than that of the reference group; the perforated fin has a Nu of 137.77, 0.7% lower than the reference; the notched fin has a Nu of 132.68, 4.4% lower than the reference. The conclusion that boundary layer disturbances are insufficient to offset the loss of effective heat transfer area is consistent with the records documented by Alpha et al.[9].

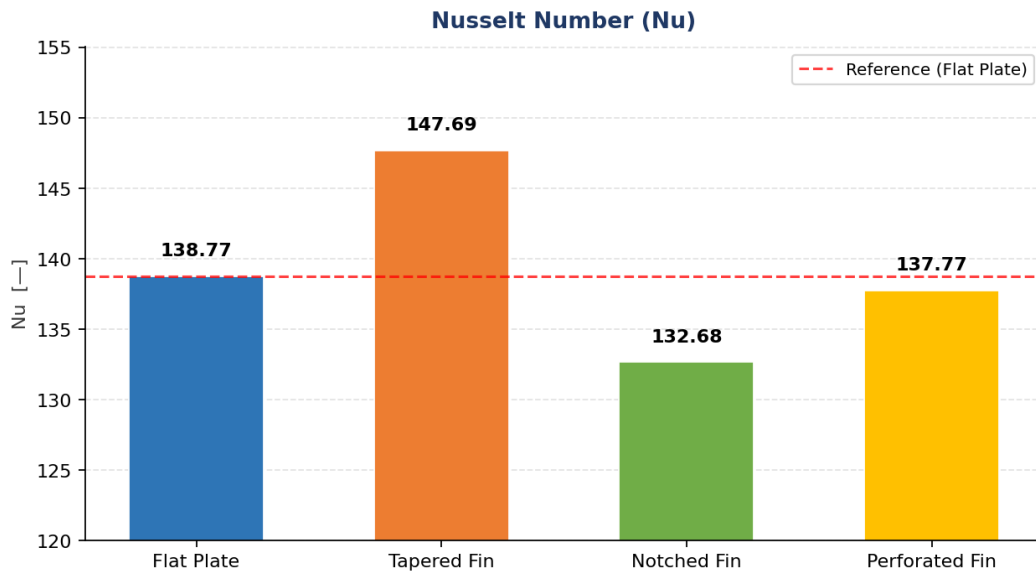


Figure 6. Nusselt number Nu. Dashed line = flat plate reference.

3.2.3 Pressure Drop

Among the three fin configurations presented in Figure 7, the conical fin has a pressure difference ΔP that reaches 5.016 Pa, which is 19% higher than the 4.217 Pa of the baseline configuration; this increase stems from the narrowed gap at the fin root. The perforated fin has a ΔP of 4.351 Pa, marking only a 3.2% rise; the lateral bypass provided by the perforations alleviates flow blockage. The notched fin records the lowest ΔP , at 4.135 Pa, which is 1.9% lower than that of the baseline. This pressure relief effect is consistent with the pressure relief effect of discontinuous fins reported by Shaeri et al. [20]

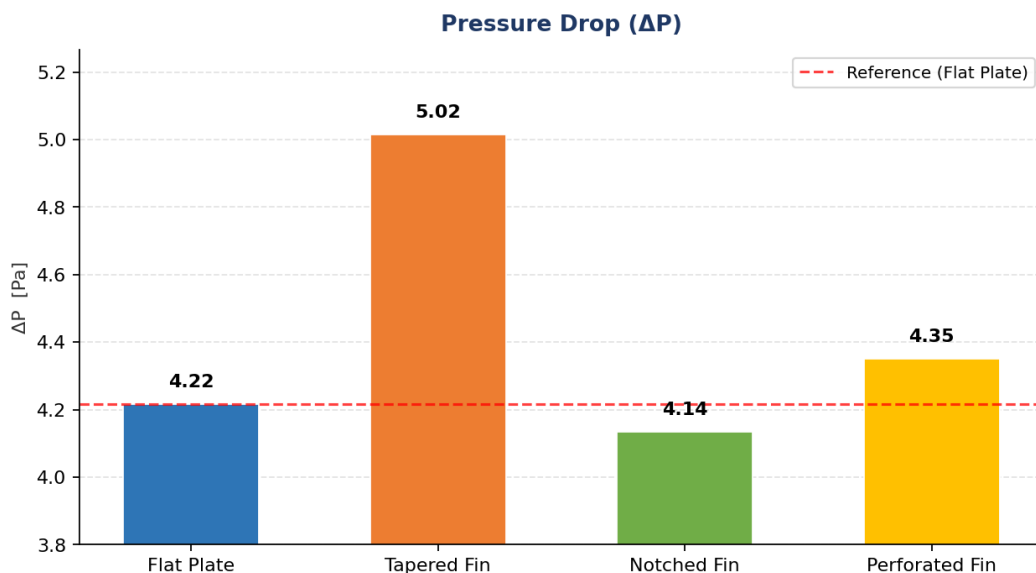


Figure 7. Pressure drop ΔP across the fin array. Dashed line = flat plate reference.

3.2.4 Performance Evaluation Criterion (PEC)

The PEC values showed in Figure 8 are the core indicator of this heat transfer performance assessment. Only the conical fin reached a PEC of 1.004, exceeding the break-even threshold of 1. Its 6.4% Nusselt number gain offset the 19% pressure drop, meeting the set standard and aligning with the conclusions of Maji et al. [9]. The porous fin and slotted fin recorded PEC values of 0.983 and 0.962 respectively, both failing to meet the standard, so their parameters require optimization.

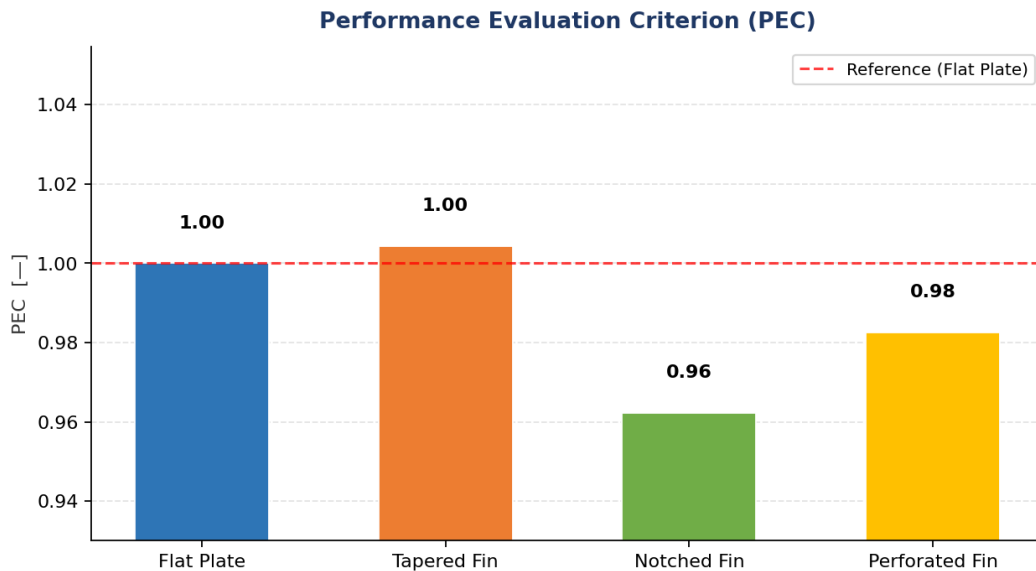


Figure 8. Performance Evaluation Criterion (PEC). PEC > 1 indicates net improvement over the flat plate reference

4. CONCLUSION

This study uses the realizable $k-\epsilon$ turbulence model built into ANSYS Fluent 2022 R1 to conduct a three-dimensional CFD study of forced air convection for four types of flat-plate fin heat sinks, and the core conclusions of this research will be elaborated in detail in subsequent sections.

1. This study's test results show that the tapered fin with a 5° draft angle is the only configuration whose performance outperforms the flat plate baseline. Its heat transfer coefficient and Nusselt number both increase by 6.4%, its PEC reaches 1.004, and its pressure drop only rises by 19%. This performance characteristic stems from the channel constriction that accelerates airflow to maintain a high local heat transfer coefficient.
2. For the perforated fins tested in this study, the convective heat transfer coefficient h decreased by 0.7%, the Nusselt number Nu saw a minor decline, the pressure drop rose by 3.2%, and the overall performance coefficient PEC was 0.983. This paper analyzes the core causes of their performance degradation.
3. The notched fin (5 alternating 8×8 mm slots) records the lowest thermal performance (h and Nu both -4.4%) despite the lowest pressure drop ($\Delta P = 4.135$ Pa), yielding $PEC = 0.962$. Flow recirculation within the notch cavities suppresses local heat transfer and the interrupted conduction path raises peak temperature to 81.1°C . Temperature profile analysis conducted in this study

confirmed that among all modified geometries, the conical profile exhibits the optimal temperature distribution, and is well-suited for electronic heat sinks applied in forced air-cooling scenarios. Future work should investigate taper angle, perforation diameter and arrangement, and notch depth as independent design variables, and extend the parametric study to higher velocities and heat fluxes.

References

- [1] D.-K. Kim, "Thermal optimization of plate-fin heat sinks with fins of variable thickness under natural convection," *Int. J. Heat Mass Transf.*, vol. 55, no. 4, pp. 752–761, 2012.
- [2] H. Mousavi, A. A. R. Darzi, M. Farhadi, and M. Omid, "A novel heat sink design with interrupted, staggered and capped fins," *Int. J. Therm. Sci.*, vol. 127, pp. 312–320, 2018.
- [3] R. Nandan, V. Arumuru, and M. K. Das, "Temperature control of electronic gadgets using novel heat sink," *Int. Commun. Heat Mass Transf.*, vol. 159, p. 108101, Dec. 2024, doi: 10.1016/j.icheatmasstransfer.2024.108101.
- [4] A. Maji, T. Deshamukhya, and G. Choubey, "Enhancement of heat dissipation rate of a heat sink with perforated fins using CFD and Swarm Intelligence," *Heat Transf.*, vol. 54, no. 1, pp. 307–329, Jan. 2025, doi: 10.1002/htj.23182.
- [5] I. E. et al. Ghandouri, "'Optimisation of the heat sink fin perforation shape using numerical methods for natural and forced convection in electronic cooling applications," *Prog. Eng. Sci.*, vol. 2, no. 2, 2025, doi: <https://doi.org/10.1016/j.pres.2025.100064>.
- [6] M. R. et al Shaeri, "Comparative numerical and experimental analysis of thermal and hydraulic performance of improved plate fin heat sinks," *Appl. Therm. Eng.*, vol. 171, 2020.
- [7] A. Arjunan and P. Kumaresan, "Investigation on Performance Characteristics of Convergent Fin Heat Sink Under Forced Convection Using CFD," 2024, pp. 537–548. doi: 10.1007/978-981-99-5990-7_46.
- [8] Haque, M.R. et al., "CFD studies on thermal performance augmentation of heat sink using perforated twisted, and grooved pin fins," *Int. J. Therm. Sci.*, vol. 182, 2022.
- [9] N. A. et al Alpha, "Experimental and numerical studies of the effect of perforation configuration on heat transfer enhancement of pin fins heat sink," *Heat Transf.*, vol. 53, pp. 2525–2555, 2024.
- [10] Els. S. ELSihy, H. Xie, T. Wang, and Z. Wang, "Multi-factor numerical research on the melting dynamics improvement of an innovative gradient finned tube latent heat storage unit," *Energy*, vol. 313, p. 133822, Dec. 2024, doi: 10.1016/j.energy.2024.133822.
- [11] A. M. Ashour, H. M. Jaffar, H. M. Ali, S. A. Kadhim, and A. Bouabidi, "Numerical and Experimental Analysis of Fin Geometry Effects on Heat Sink Performance in Thermoelectric Air-Cooling Systems," *Heat Transf.*, vol. 55, no. 2, pp. 1265–1279, Mar. 2026, doi: 10.1002/htj.70135.
- [12] J. et al Li, "Study and optimization of ribbed flat-plate fin heat sink based on placoid scale shape," *Int. J. Heat Fluid Flow*, vol. 110, p. 109590, Dec. 2024, doi: 10.1016/j.ijheatfluidflow.2024.109590.
- [13] A. Maji, D. Bhanja, and P. K. Patowari, "Numerical investigation on heat transfer enhancement of heat sink using perforated pin fins with inline and staggered arrangement," *Appl. Therm. Eng.*, vol. 125, pp. 596–616, 2017.
- [14] F.-T. Zohora, M. R. Haque, N. M. Chowdhury, M. K. Fahad, and N. F. Ifraj, "Optimization of



hydrothermal performance in industrial heat sinks with innovative perforated pin fin designs: A numerical approach,” *Heliyon*, vol. 11, no. 1, p. e41496, Jan. 2025, doi: 10.1016/j.heliyon.2024.e41496.

- [15] M. et al Muneeshwaran, “Topological structures for microchannel heat sink applications — a review,” *Manuf. Rev.*, vol. 10, p. 31, Oct. 2023, doi: 10.1051/mfreview/2022029.
- [16] Pires-Fonseca, W.D. and Carrasco-Altemani, C.A., “Experimental and numerical investigation of flat plate fins and inline strip fins heat sinks,” *Rev. Fac. Ing. Univ. Antioquia*, 2023, doi: <https://doi.org/10.17533/udea.redin.20221000>.
- [17] W. Versteeg, H. K., & Malalasekera, *An Introduction to Computational Fluid Dynamics: The Finite Volume Method*, 2nd ed. pearson Education, 2007.
- [18] F. P. et al Incropera, *Fundamentals of Heat and Mass Transfer*, 7th ed. John Wiley & Sons, 2011.
- [19] T.-H. et al Shih, “A new k-epsilon eddy viscosity model for high Reynolds number turbulent flows,” *Comput. Fluids*, vol. 24, no. 3, pp. 227–238, 1995.
- [20] M. R. Shaeri and M. Yaghoubi, “Numerical analysis of turbulent convection heat transfer from an array of perforated fins,” *Int. J. heat fluid flow*, vol. 30, no. 2, pp. 218–228, 2009.